**Actuation Porphyrin-Containing Dielectric Silicone Elastomers**

Cody B. Gale,[a] Michael A. Brook*[a] and Anne Ladegaard Skov*[b]

**Supporting Information**

## Characterization of Zn-TPMP

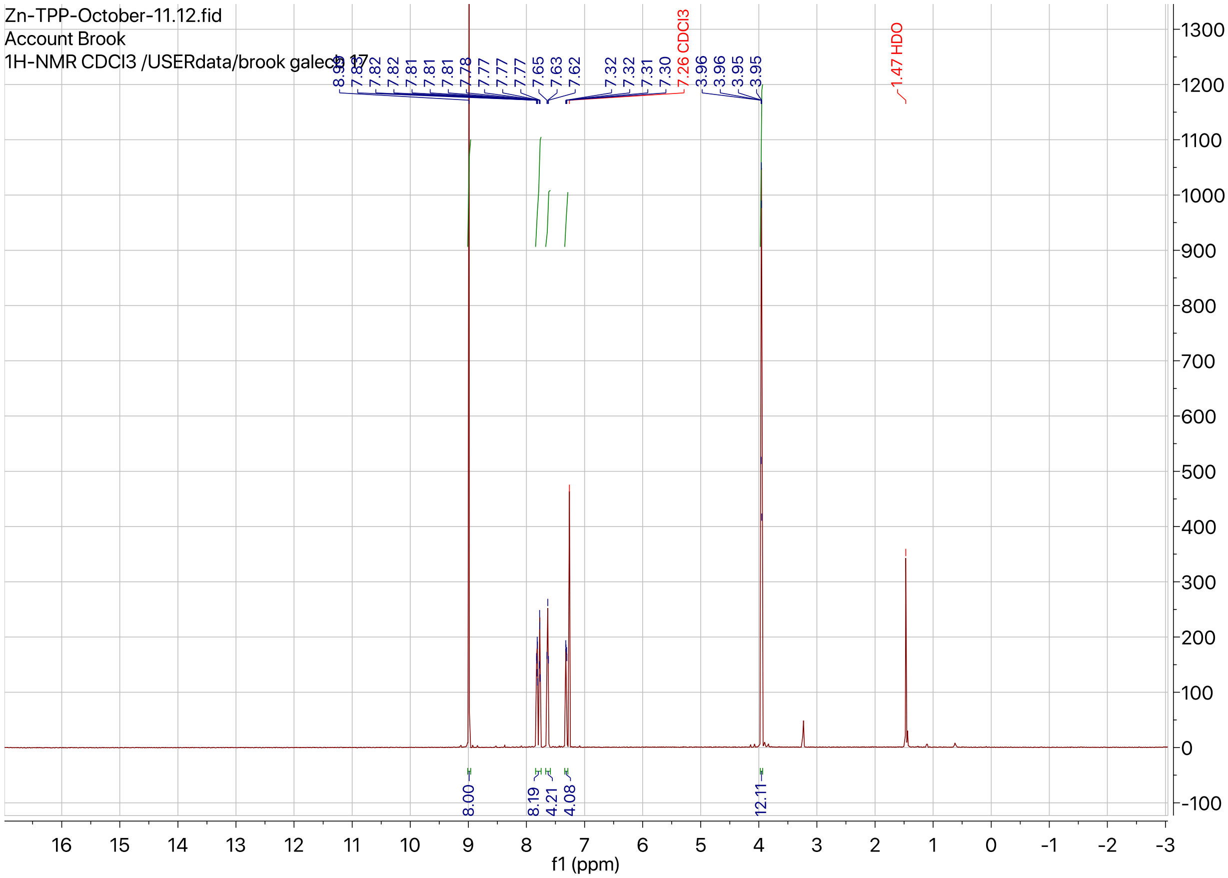


Figure S1: $^{1}$H-NMR of Zn-TPMP.

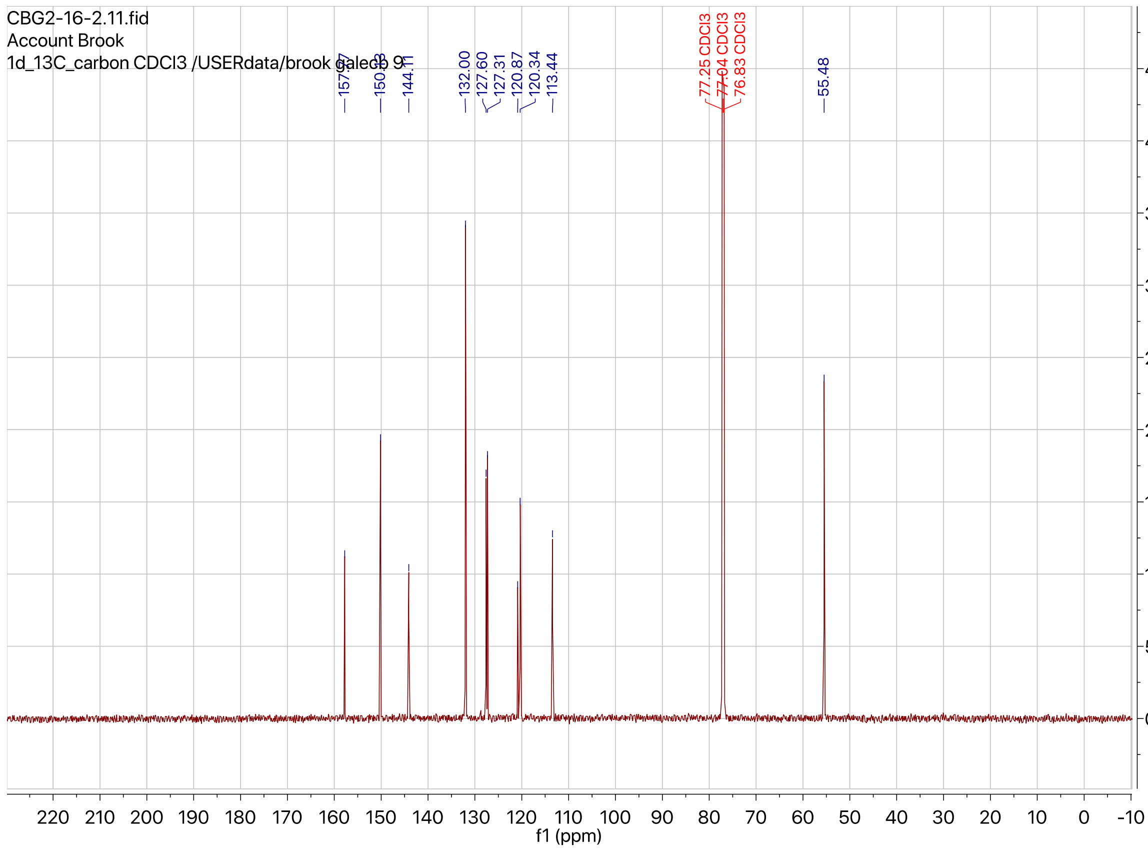


Figure S2: $^{13}$C-NMR of Zn-TPMP.

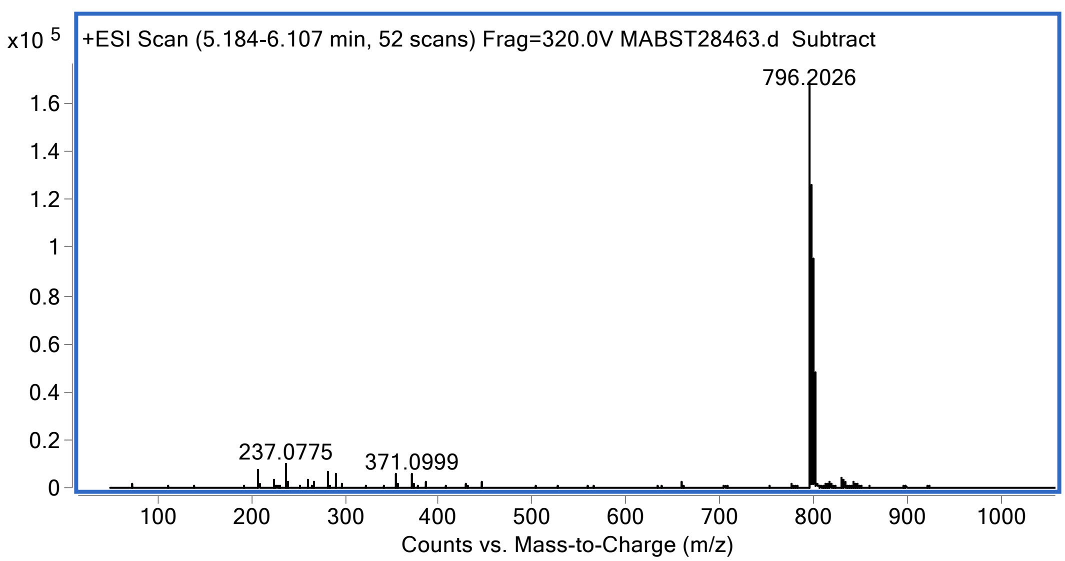


Figure S3: ESI-MS of Zn-TPMP.

**Characterization of Zn-TPMP-Bis-H**

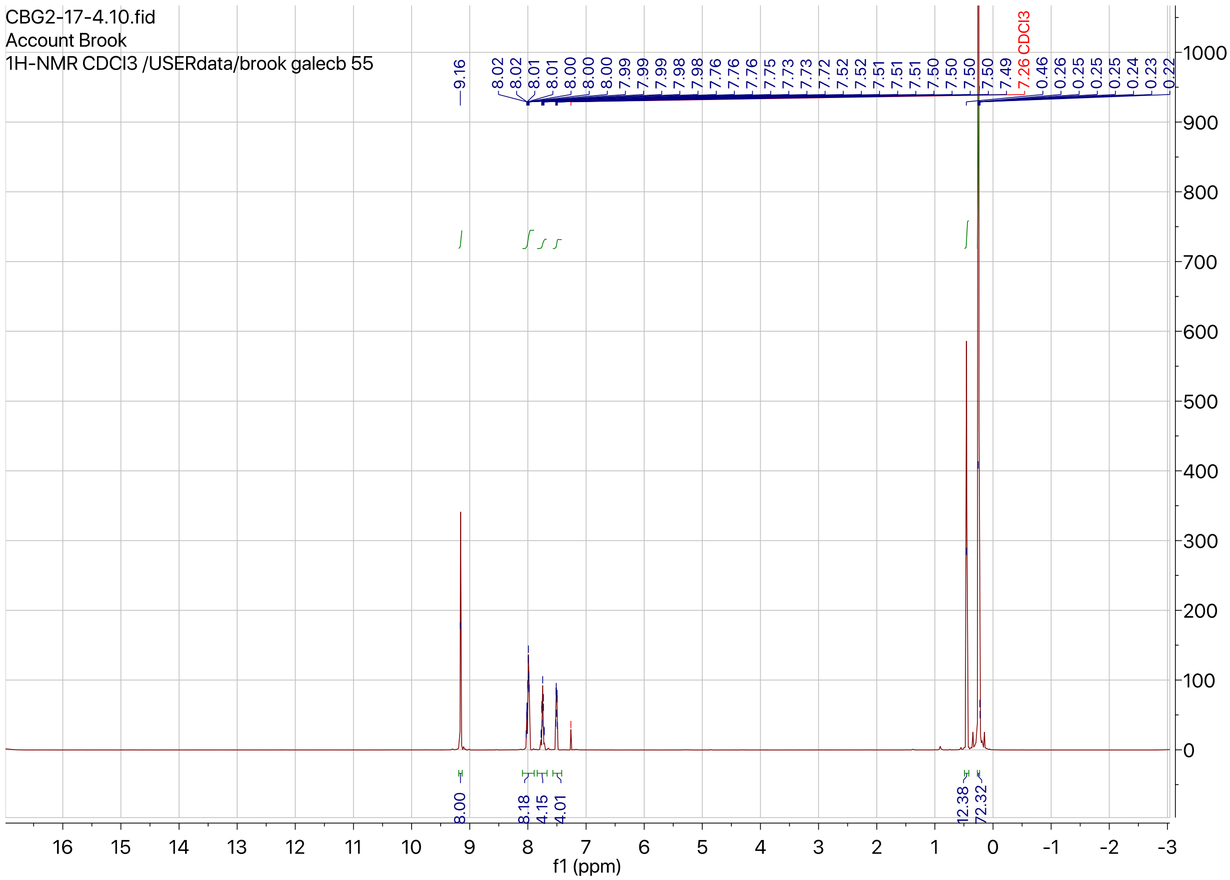


Figure S4: $^{1}$H-NMR of Zn-TPMP-Bis-H

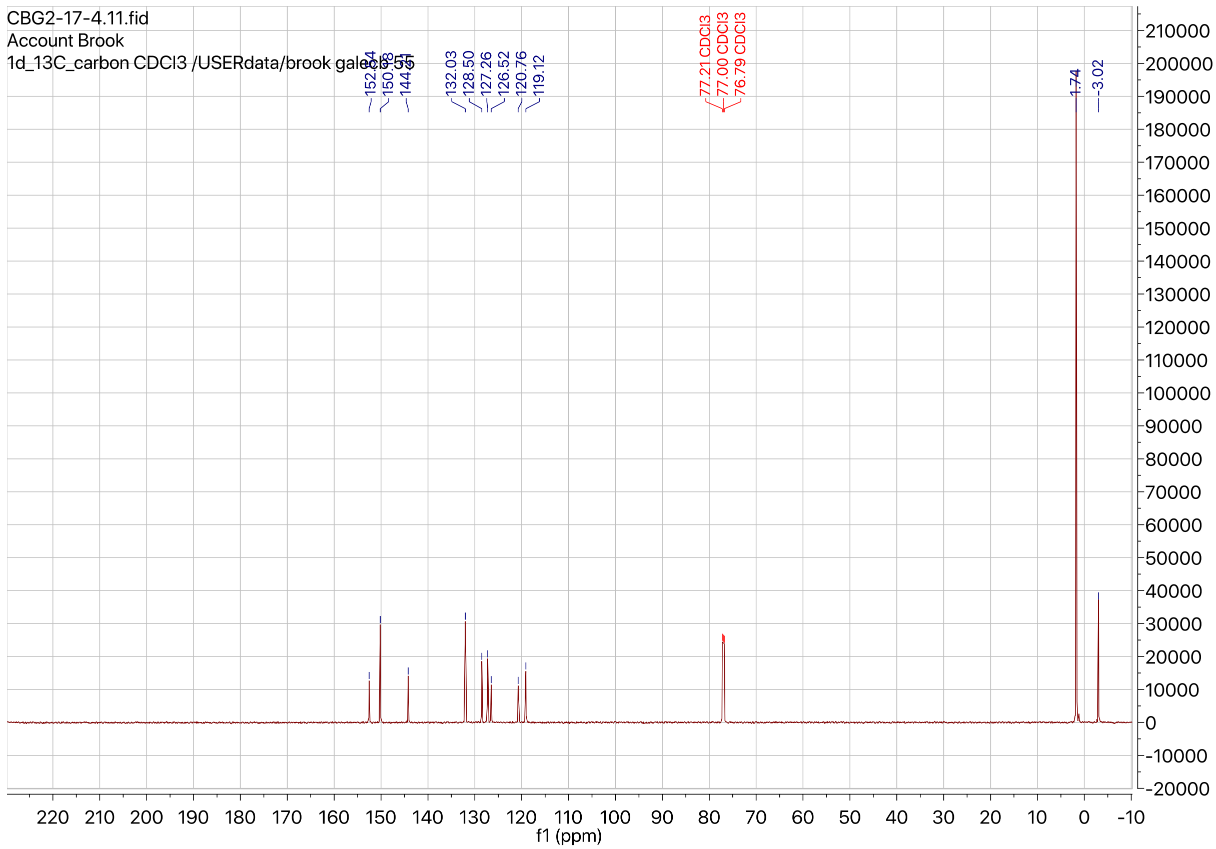


Figure S5: $^{13}$C-NMR of Zn-TPMP-Bis-H.

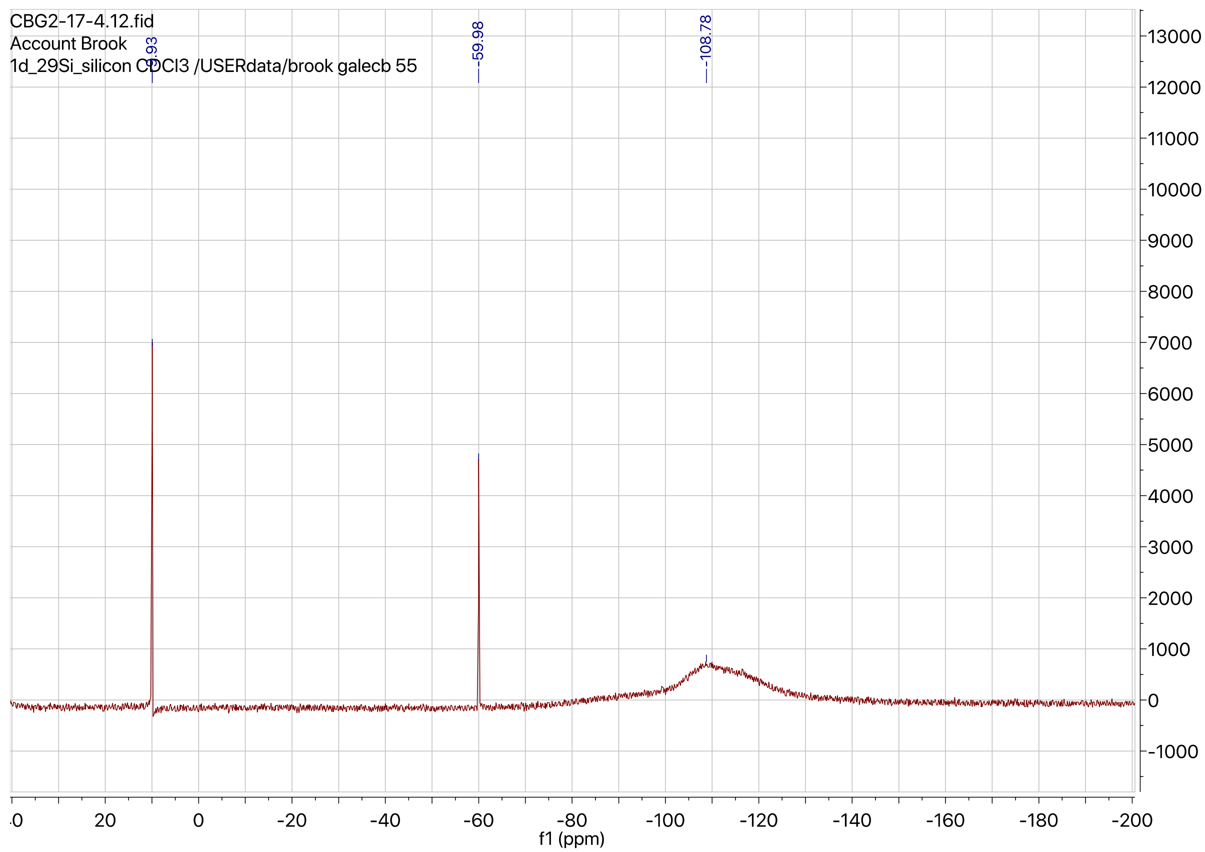


Figure S6: $^{29}$Si NMR of Zn-TPMP-Bis-H.

Figure S1:

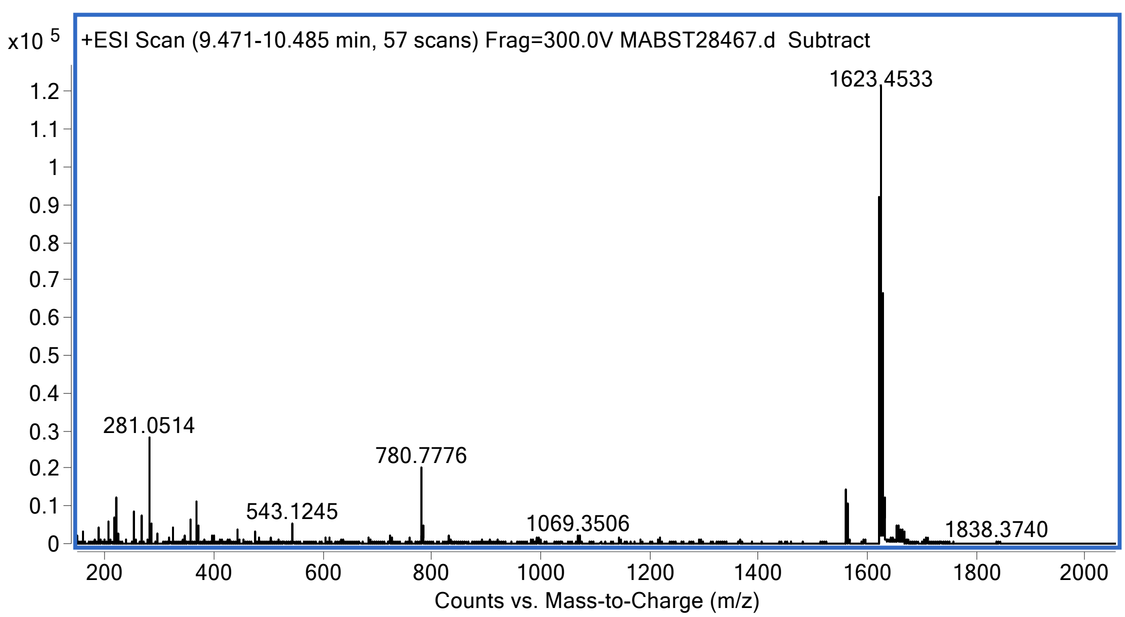


Figure S7: ESI-MS of Zn-TPMP-Bis-H.

**Dielectric Properties of Zn-TPMP Elastomers**

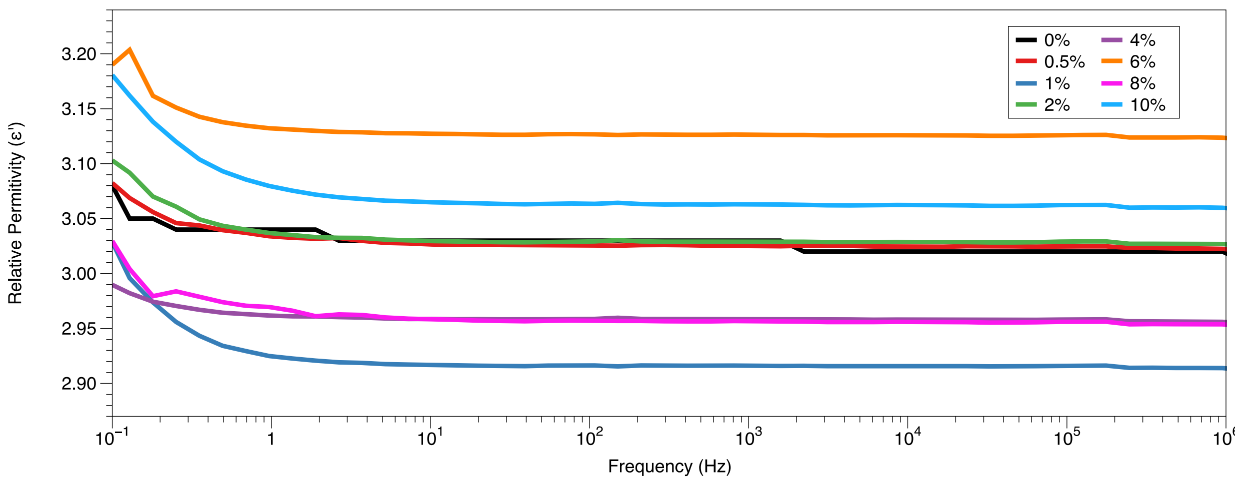


Figure S8: Relative permittivity of Zn-TPMP in HMS-301+DMS-V22 platinum cure system.

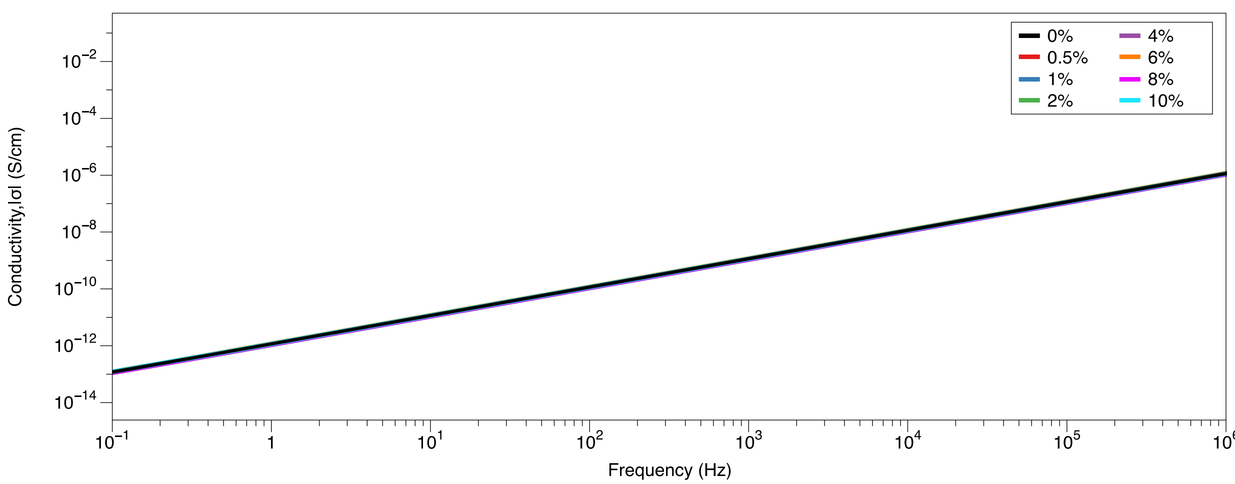


Figure S9: Conductivity of Zn-TPMP in HMS-301+DMS-V22 platinum cure system.

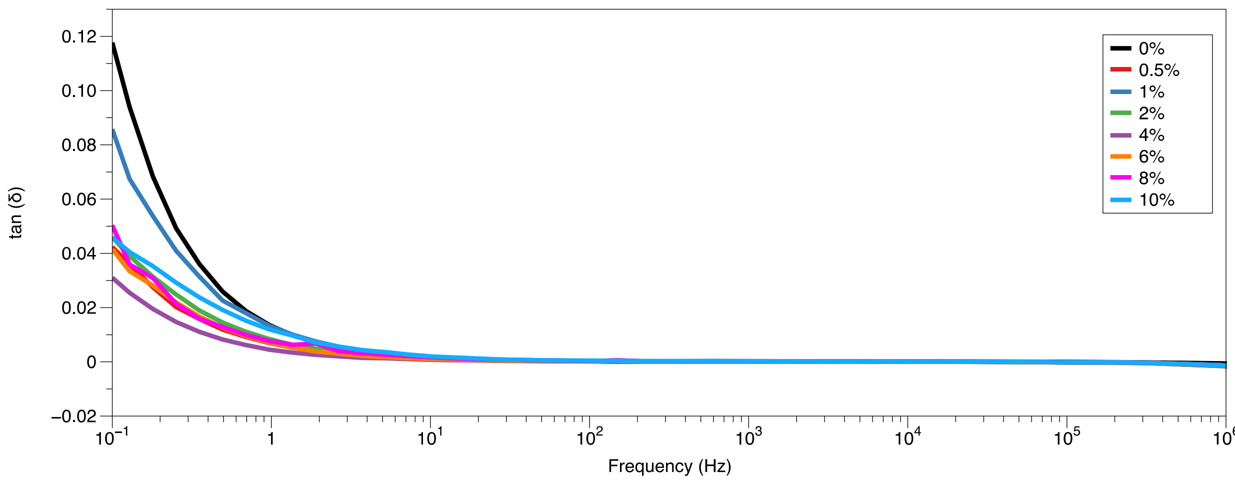


Figure S10: Dielectric loss of Zn-TPMP in HMS-301+DMS-V22 platinum cure system.

**Dielectric Properties of Zn-TPMP-Bis-H Elastomers**

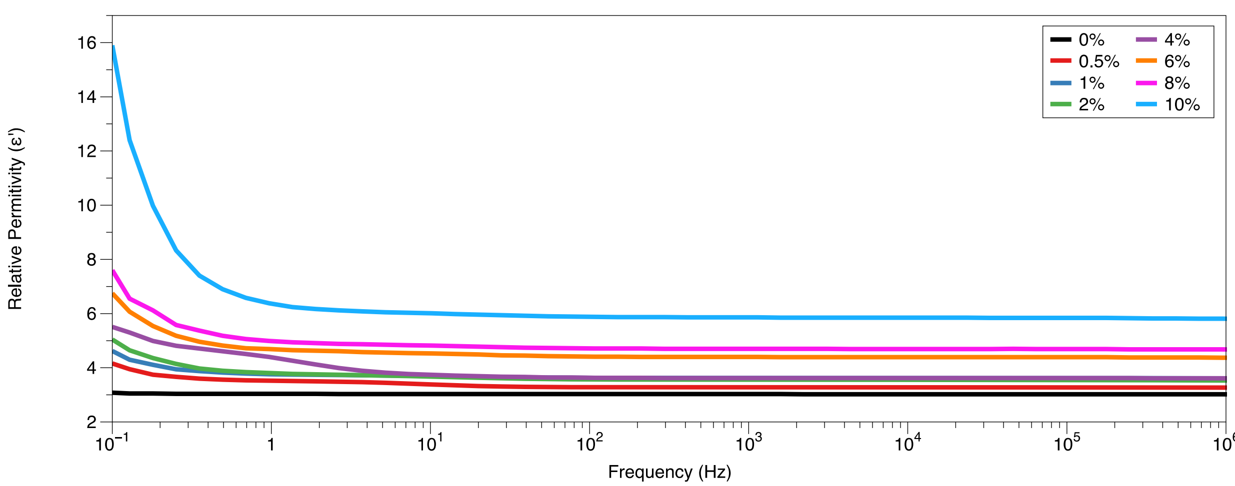


Figure S11: Relative permittivity of Zn-TPMP-Bis-H in HMS-301+DMS-V22 platinum cure system.

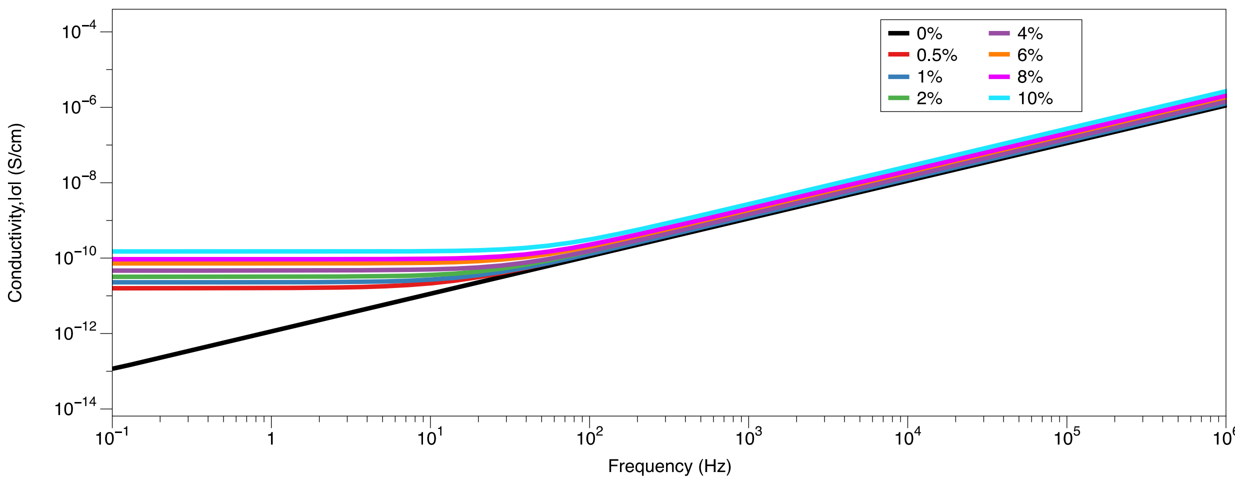

Figure S12: Conductivity of Zn-TPMP-Bis-H in HMS-301+DMS-V22 platinum cure system.

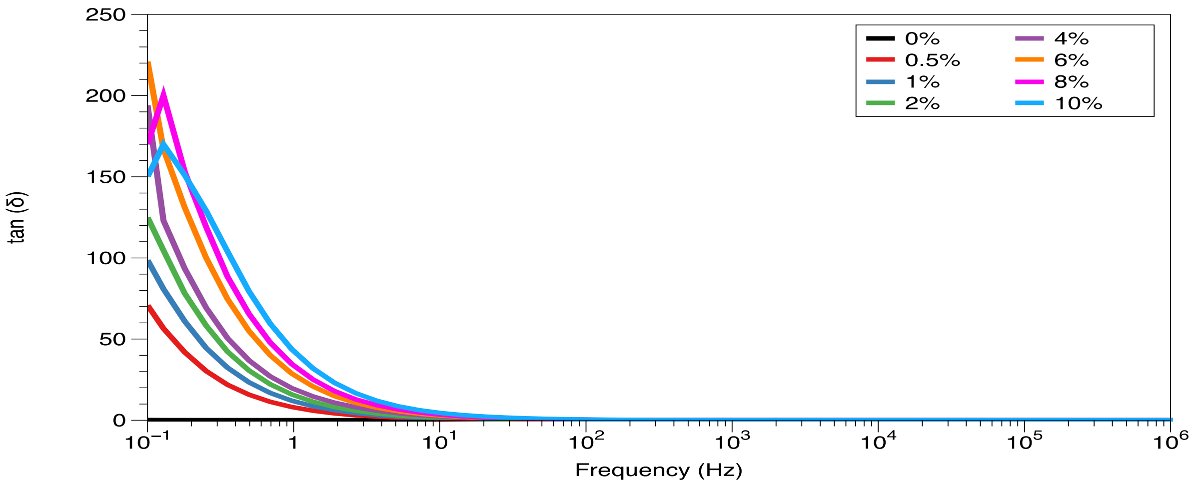

Figure S13: Dielectric loss of Zn-TPMP-Bis-H in HMS-301+DMS-V22 platinum cure system.

**Dielectric Properties of Elastosil 625 Zn-TPMP-Bis-H Elastomers**

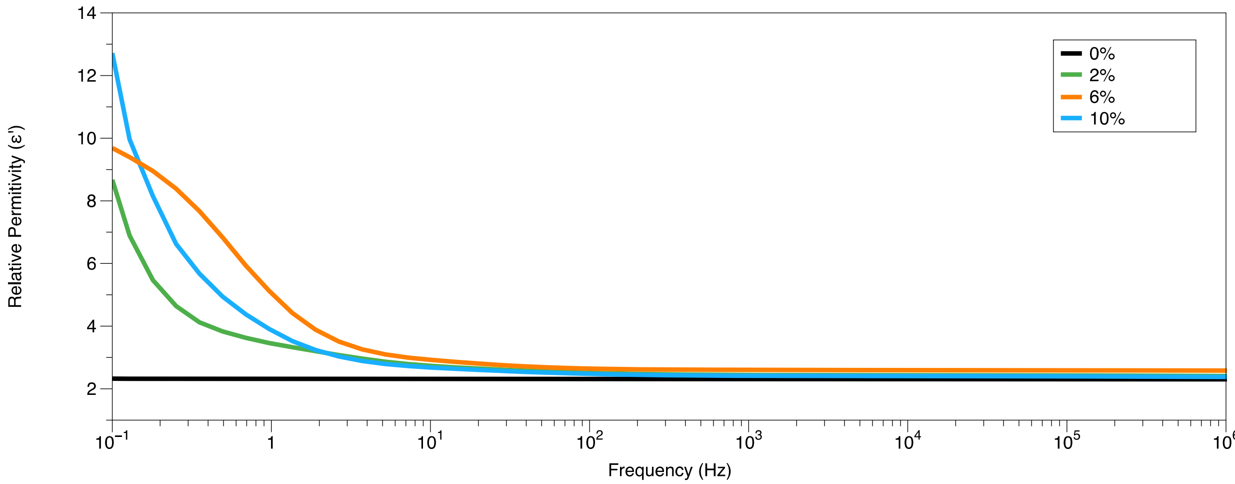


Figure S14: Relative permittivity of Zn-TPMP-Bis-H in Elastosil 625.

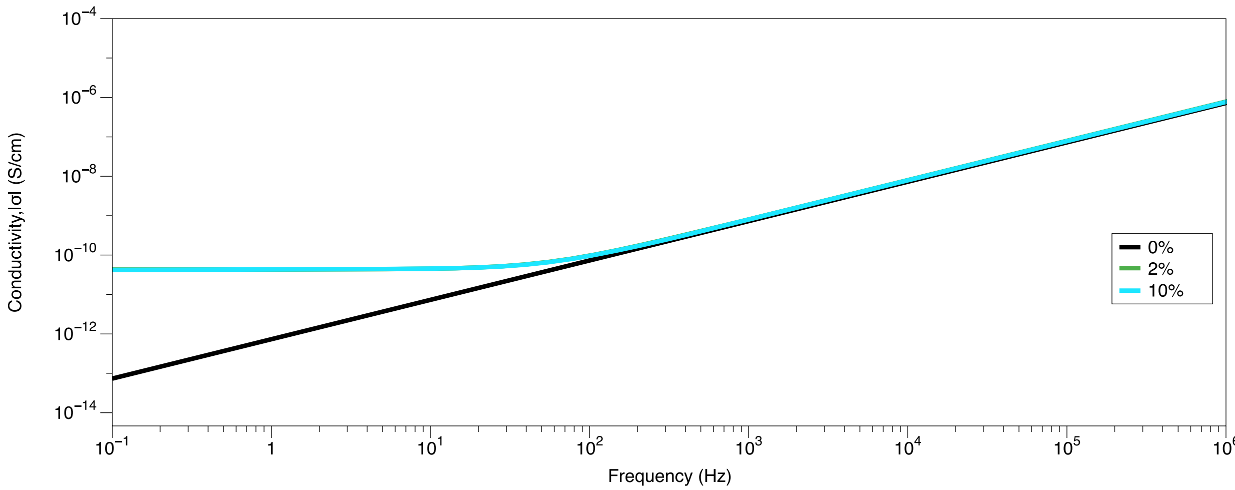


Figure S15: Conductivity of Zn-TPMP-Bis-H in Elastosil 625.

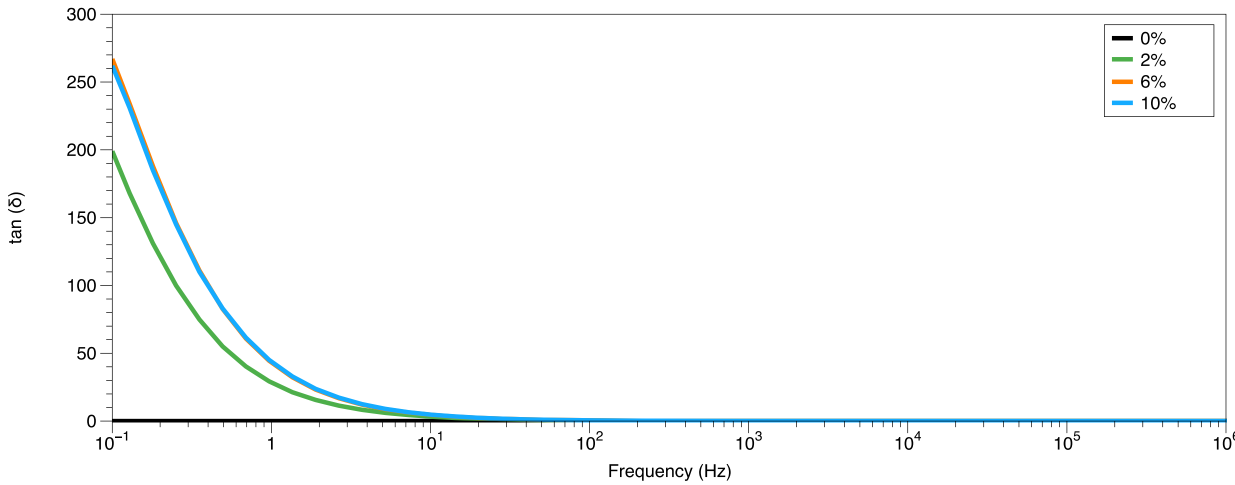

Figure S16: Dielectric loss of Zn-TPMP-Bis-H in Elastosil 625.

Table S1: Electrical breakdown results for Elastosil 625 0% Zn-TPMP-Bis-H.

| | | |
|---|---|---|
| Sample | | Elastosil 625 0% |
| Sample normal thickness (μμm) measured with optical microscope | | 107 |
| Thickness measured with gauge (μm) | Breakdown voltage (kV) | Field Strength (V/μm) |
| 107 | 10.2 | 95.6 |
| 107 | 11.1 | 104 |
| 107 | 10.6 | 99.3 |
| 107 | 10.0 | 93.5 |
| 105 | 10.0 | 95.6 |
| 106 | 11.3 | 107 |
| 107 | 10.9 | 102 |
| 105 | 10.5 | 100 |
| 107 | 10.8 | 101 |
| 107 | 10.1 | 94.3 |
| 108 | 10.0 | 92.8 |
| 107 | 10.4 | 97.2 |
| Average Field Strength (V/μm) | | 98.4 |
| STDEV | | 4.11 |
| $\beta$ | | 26.6 |
| $\eta$ | | 100 |
| $R^2$ | | 0.886 |

Table S2: *Electrical breakdown results for Elastosil 625 2% Zn-TPMP-Bis-H*

| Sample | | Elastosil 625 2% |
|---|---|---|
| Sample normal thickness (μm) measured with optical microscope | | 116 |
| Thickness measured with gauge (μm) | Breakdown voltage (kV) | Field Strength (V/μm) |
| 117 | 6.66 | 56.9 |
| 116 | 6.69 | 57.7 |
| 116 | 6.58 | 56.7 |
| 116 | 6.52 | 56.2 |
| 115 | 6.98 | 60.7 |
| 115 | 7.33 | 63.7 |
| 117 | 7.4 | 63.2 |
| 115 | 6.74 | 58.6 |
| 117 | 7.16 | 61.2 |
| 117 | 7.02 | 60.0 |
| 115 | 7 | 60.9 |
| 115 | 6.98 | 60.7 |
| Average Field Strength (V/μm) | | 59.7 |
| STDEV | | 2.39 |
| $\beta$ | | 27.86 |
| $\eta$ | | 61 |
| $R^2$ | | 0.9 |

Table S3: Electrical breakdown results for Elastosil 625 6% Zn-TPMP-Bis-H.

| Sample | | Elastosil 625 6% |
|---|---|---|
| Sample normal thickness (μm) measured with optical microscope | | 102 |
| Thickness measured with gauge (μm) | Breakdown voltage (kV) | Field Strength (V/μm) |
| 102 | 6.08 | 59.6 |
| 100 | 5.8 | 58.0 |
| 101 | 5.88 | 58.2 |
| 102 | 5.81 | 56.9 |
| 103 | 5.72 | 55.5 |
| 102 | 5.71 | 55.9 |
| 103 | 5.72 | 55.5 |
| 102 | 5.94 | 58.2 |
| 100 | 5.32 | 53.2 |
| 102 | 6.13 | 60.1 |
| 102 | 6.12 | 60 |
| 102 | 5.69 | 55.8 |
| Average Field Strength (V/μm) | | 57.3 |
| STDEV | | 2.1 |
| $\beta$ | | 31.9 |
| $\eta$ | | 58 |
| $R^2$ | | 0.94 |

Table S4: Electrical breakdown results for Elastosil 625 10% Zn-TPMP-Bis-H.

| | | |
|---|---|---|
| Sample | | Elastosil 625 10% |
| Sample normal thickness (μm) measured with optical microscope | | 97 |
| Thickness measured with gauge (μm) | Breakdown voltage (kV) | Field Strength (V/μm) |
| 103 | 5.19 | 50.4 |
| 103 | 5.41 | 52.5 |
| 107 | 4.97 | 46.4 |
| 103 | 5.15 | 50.0 |
| 105 | 5.25 | 50.0 |
| 107 | 5.00 | 46.7 |
| 105 | 4.97 | 47.3 |
| 105 | 5.18 | 49.3 |
| 105 | 5.27 | 50.2 |
| 103 | 5.59 | 54.3 |
| 103 | 5.50 | 53.4 |
| 103 | 5.48 | 53.2 |
| Average Field Strength (V/μm) | | 50.3 |
| STDEV | | 2.63 |
| β | | 22.0 |
| η | | 52.7 |
| $R^2$ | | 0.912 |

**Rheology Results/ Tensile Tests Results**

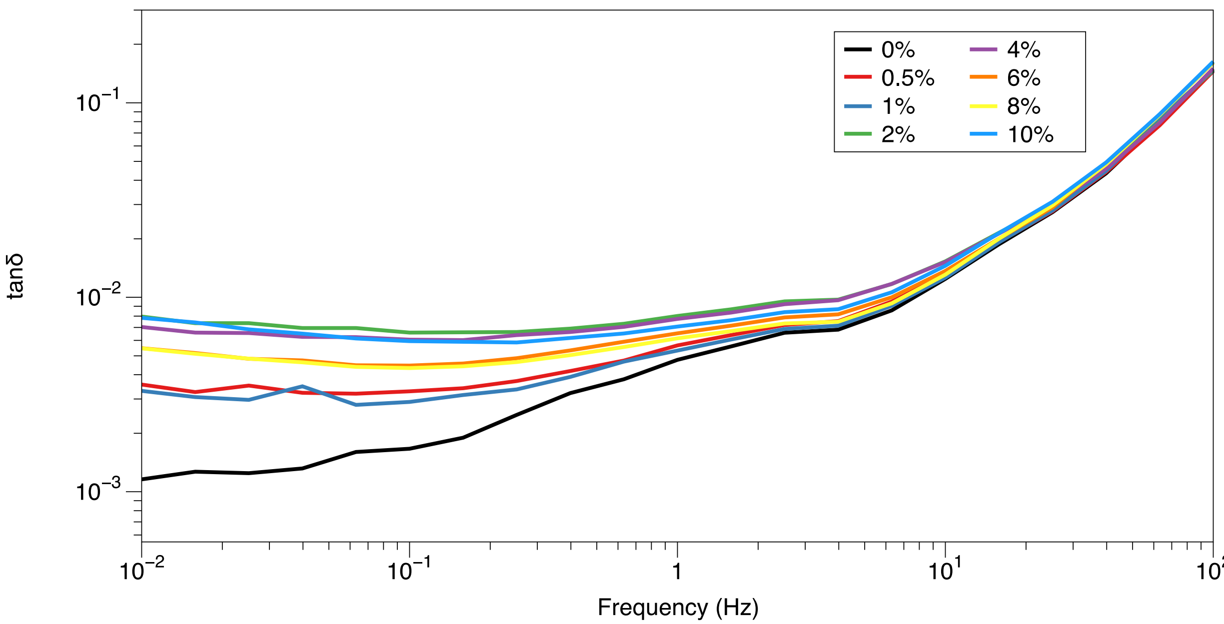


Figure S17: tan(δ) of Zn-TPMP elastomers, homemade formulation @25°C

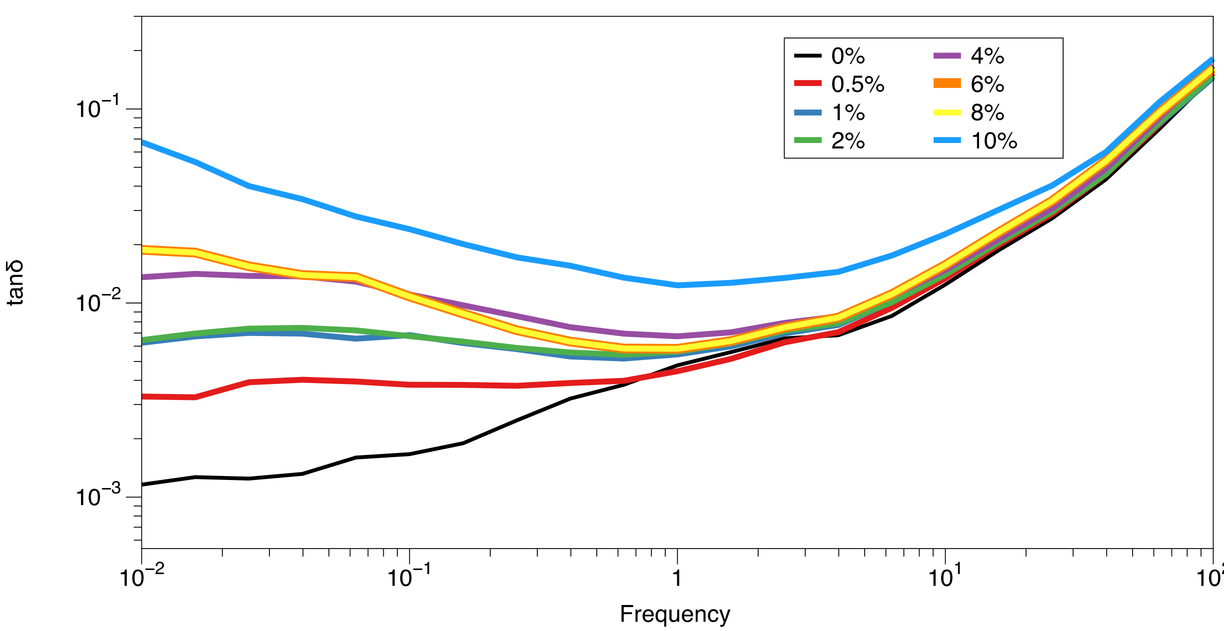


Figure S18: tan(δ) of Zn-TPMP-Bis-H elastomers, homemade formulation @25°C.

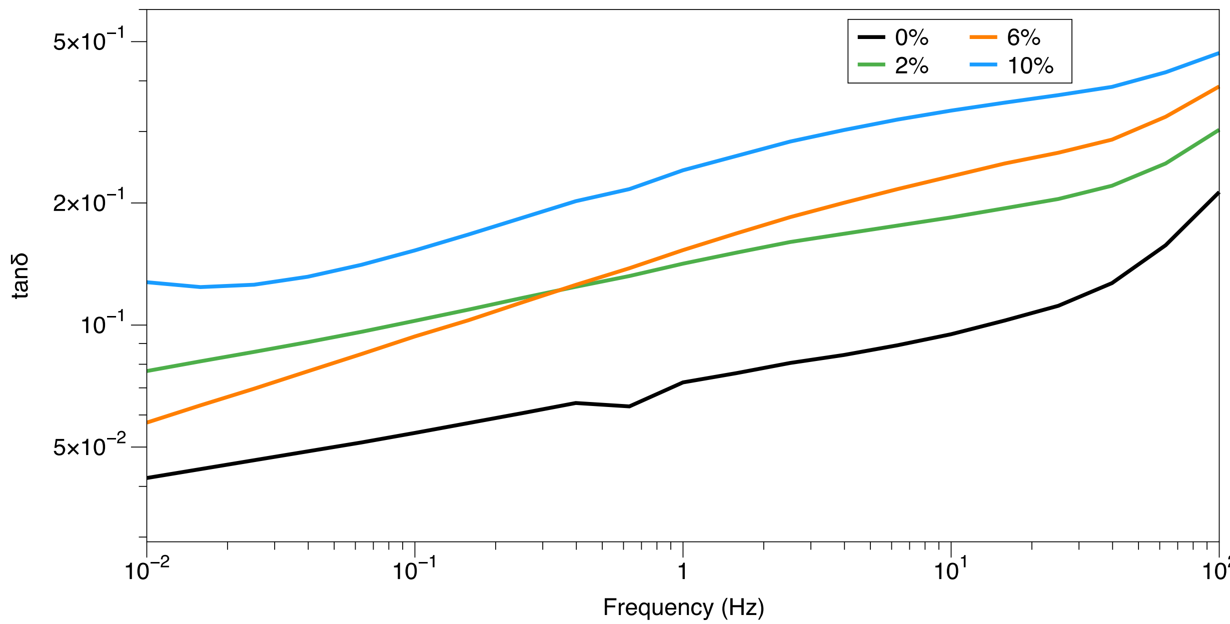

Figure S19: tan(δ) of Zn-TPMP-Bis-H elastomers, Elastosil 625 @25°C.

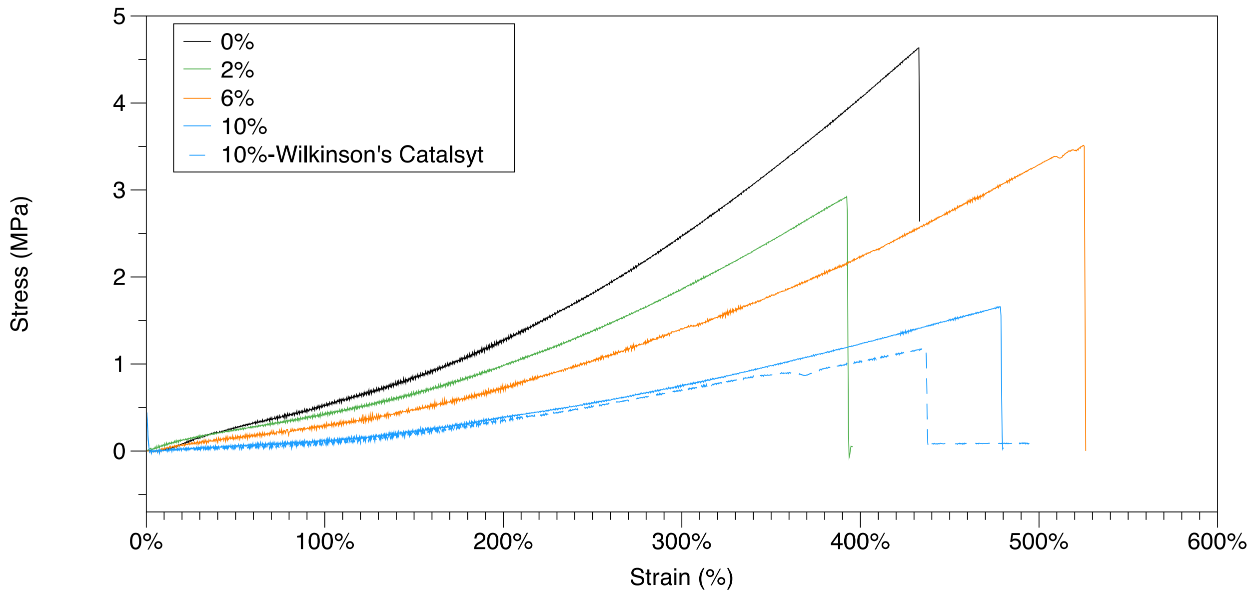

Figure S20: Stress-Strain curves for Elastosil 625 elastomers.

**Elastomer Curing-Elastosil 625**

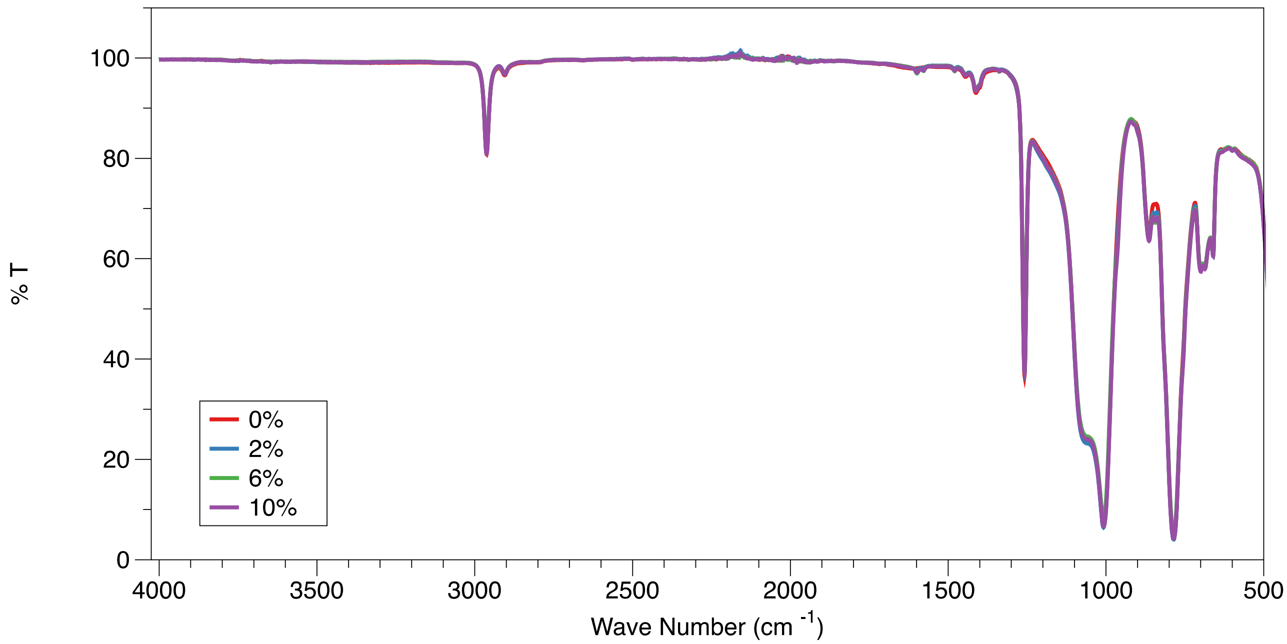

Figure S21: IR of Elastosil 625 samples containing varying percentages of Zn-TPMP-Bis-H.

It was important to establish whether the differences in mechanical properties of the samples containing 6 and 10% porphyrin, were a result of incomplete curing. IR spectroscopy was used to probe the samples for unreacted Si-H groups, which would indicate that that the porphyrin was quenching the catalyst. The IR spectra of the samples was obtained no peaks in the 2080-2280 cm$^{-1}$ region, indicative of unreacted Si-H could be detected. Secondary analysis of the samples via $^{1}$H-NMR was not informative as the signals corresponding to Si-$CH_3$ protons overwhelmed all other signals.

Table S5: Shore OO data for Elastosil 625 samples.

| % Zn-TPMP-Bis-H | Shore OO |
|---|---|
| 0 | 75 |
| 2 | 67 |
| 6 | 55 |
| 10 | 37 |

**Phase Separation/ Oil Migration**

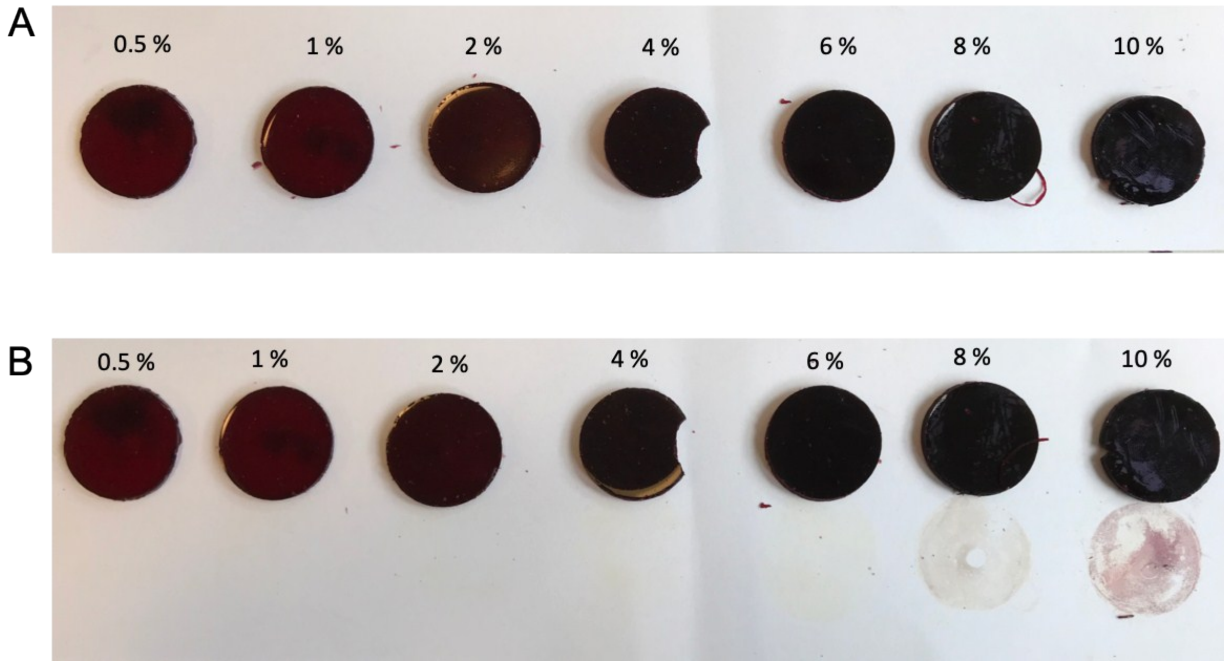


Figure S22: A) Zn-TPMP-Bis-H elastomers in homemade formulation placed on paper. B) Residue of elastomers left behind on paper after application of 2 kg weight to each elastomer.

A

B

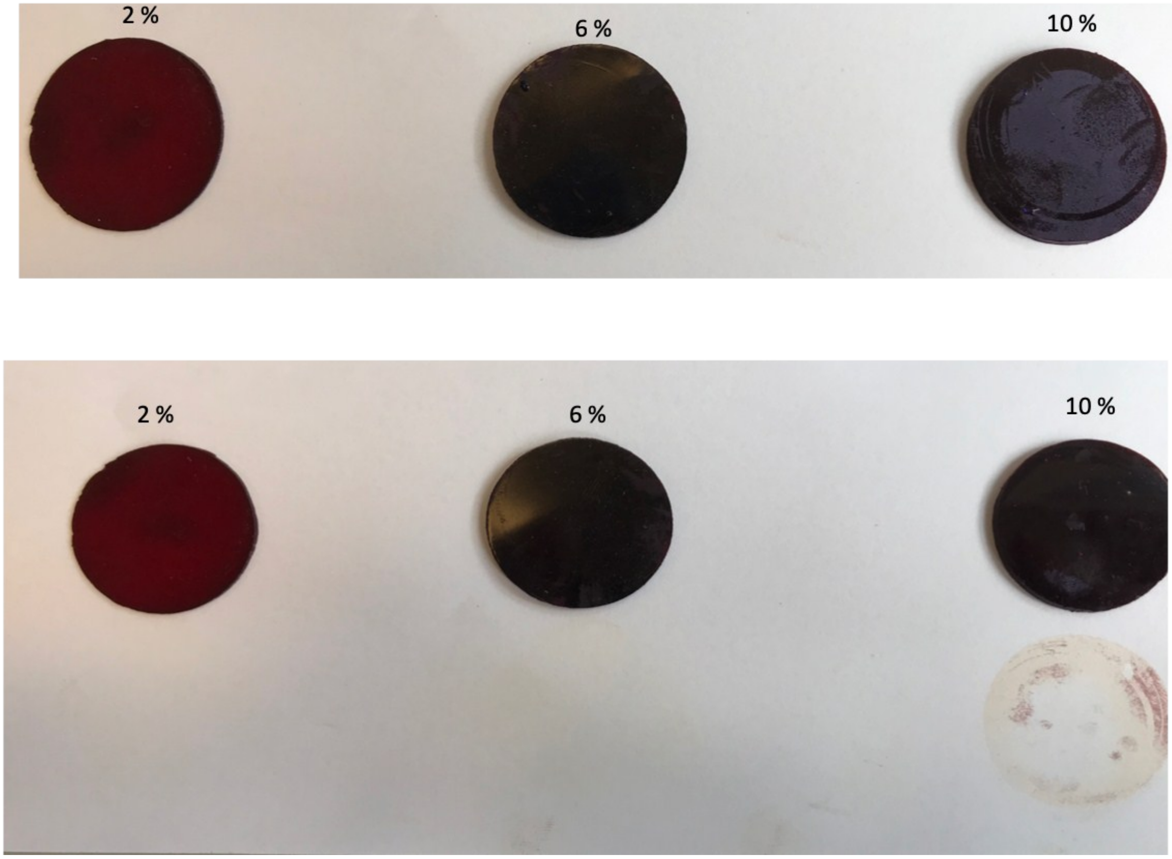


Figure S23: A) Zn-TPMP-Bis-H elastomers in Elastosil 625 placed on paper. B) Residue of elastomers left behind on paper after application of 2 kg weight to each elastomer.